Reconstruction of D^0 meson in d+Au collisions at $\sqrt{s_{\mathrm{NN}}} = 200$ GeV by the STAR experiment

Lukáš Kramárik for the STAR collaboration
Department of Physics
Faculty of Nuclear Sciences and Physical Engineering
Czech Technical University in Prague
Břehová 7, 115 19 Prague 1, Czech Republic

E-mail: `lukas.kramarik@fjfi.cvut.cz`

February 2020

Abstract. Owing to their large masses, charm quarks are predominantly produced through initial hard scatterings in heavy-ion collisions. Therefore, they can serve as penetrating probes to study the intrinsic properties of the hot medium created in heavy-ion collisions. However, Cold Nuclear Matter effects can also affect the charm quark production in nuclear collisions with respect to p+p collisions. These effects can be measured in small collision systems such as d/p+Au.

In these proceedings, D^0 meson reconstruction in d+Au collisions at $\sqrt{s_{\mathrm{NN}}} = 200$ GeV at the STAR experiment is described. Thanks to the excellent impact parameter resolution provided by the Heavy Flavor Tracker detector, $D^0(\overline{D^0})$ mesons are topologically reconstructed from their hadronic decay channel $D^0(\overline{D^0}) \rightarrow K^-\pi^+(K^+\pi^-)$. The Boosted Decision Trees machine learning algorithm from the TMVA package is applied in order to improve signal/background separation.

1. Introduction

In ultrarelativistic collisions of heavy ions, hot and dense nuclear matter, quark-gluon plasma (QGP), could be created [1]. Since heavy-flavor (charm and beauty) quarks are produced in hard scatterings at the early stage of such collisions [2], they experience the entire evolution of the system including the QGP phase. At Relativistic Heavy Ion Collider (RHIC), strong suppression of open charm mesons at high transverse momentum (p_{T}) in the 0—10% most central gold-gold (Au+Au) collisions was measured [3], indicating substantial energy loss of charm quarks in the hot medium. In addition, it was measured that charm quarks exhibit collective behavior [4], that reflects the degree of thermalization of charm quarks in the medium and carries information about the transport properties of the QGP.

However, for more detailed study of the QGP effects on produced particles, quantitative understanding of the effects of the heavy nuclei in the initial stages of collisions is needed. These so-called Cold Nuclear Matter effects includes mainly modification of parton distribution functions of nucleons in colliding nuclei [5, 6], multiple scatterings of the partons by the dense target and parton scatterings in the nucleus, resulting in their energy loss and to the broadening of the transverse momentum (Cronin effect) [7, 8].

CNM effects are investigated in the asymmetric collisions of protons or deuterons with nuclei. At Large Hadron Collider (LHC) in CERN, CNM effects on D^0 production were studied in proton-lead (p+Pb) collisions. ALICE experiment measured, that D^0 production in such events is not significantly modified compared to proton-proton collisions [9]. However, CMS collaboration measured significant collective behavior (large elliptic flow v_2) of D^0 mesons in p+Pb collisions at $\sqrt{s_{\rm NN}} = 8.16$ TeV [10]. At RHIC, CNM effects are accessible via proton-gold (p+Au) and deuteron-gold (d+Au) collisions. Energy density in such collisions is expected to be too low to create thermalized medium, nevertheless the dense nuclear environment alters colliding nucleons.

Reconstruction of open charm D^0 mesons described in these proceedings was done in data from d+Au collisions at $\sqrt{s_{\rm NN}} = 200$ GeV. These were measured by the Solenoidal Tracker at RHIC (STAR), situated in Brookhaven National Laboratory (BNL) in the USA. Topological reconstruction of the hadronic decay of D^0 meson to K^- and π^+ with branching ratio 3.89 ± 0.04 % [11] is used. Shown results are for combined D^0 and $\overline{D^0}$ mesons, thus both unlike-sign combinations of pion and kaon ($K^-\pi^+$ and $K^+\pi^-$) are considered to be correct charge combinations. Furthermore, the Boosted Decision Trees (BDT) machine learning algorithm from the Toolkit for Multivariate Data Analysis (TMVA) package [12] is applied in order to improve separation of signal and background $K\pi$ pairs.

2. Experimental setup - STAR detector

STAR consists of multiple subdetectors, that are able to track and identify charged particles down to very low $p_{\rm T}$ at mid-rapidity ($|\eta| < 1$) with the full azimuthal coverage. STAR's main tracking sub-system is the Time Projection Chamber (TPC) [13], a gaseous detector that identifies particles via specific energy loss in it and determines momentum from the curvature of their trajectories in the 0.5 Tesla solenoidal field.

Another detector, that was developed to improve the particle identification capability for tracks with momenta between 0.6 and 3 GeV/c, is the Time of Flight (TOF) [14]. It measures the velocity of a particle, β, by measuring the time interval that the particle needs to reach the TOF from the point of the collision. Time of a collision is detected with fast Vertex Position Detectors (VPD) [15], that detects particles produced in forward directions.

For the analysis presented in these proceedings, the Heavy Flavor Tracker (HFT) [16] detector has a great importance. It is the high-precision silicon vertex detector installed at the center of the STAR for data taking in years 2014–2016. It greatly improves the track pointing resolution and enables the topological reconstruction of the secondary vertices of open charm hadron decays through hadronic channels. It consists of three silicon detectors - the PIXEL made of two layers of Monolithic Active Pixel Sensors, Intermediate Silicon Tracker (IST) and Silicon Strip Detector (SSD). The HFT achieves excellent distance of the closest approach (DCA) resolution, e.g. 30 μm for kaons at transverse momentum $p_{\mathrm{T}} = 1.5$ GeV/c [16].

3. Event and track selection

In 2016, approximately 350 million of d+Au minimum bias collisions at $\sqrt{s_{\mathrm{NN}}} = 200$ GeV were recorded. Only events that are well reconstructed in the HFT geometric acceptance are accepted for this analysis. This is assured by requiring that the reconstructed position of the primary vertex in the beam direction from the center of detector (V_z) is less than 6 cm. To reduce pile-up from multiple events, events with correlated primary vertices reconstructed by the TPC and by the VPD ($|V_{z,\mathrm{TPC}} - V_{z,\mathrm{VPD}}| < 6$ cm) are further analyzed.

For this analysis, reconstructed tracks with pseudorapidity $|\eta| < 1$ and $p_{\mathrm{T}} > 0.15$ GeV/c are used. They are also required to have at least 15 measured points in the TPC out of maximum 45, hits in both layers of PIXEL detector and at least one hit in IST or SSD layers of the HFT. Particles are identified using the specific energy loss $\mathrm{d}E/\mathrm{d}x$ in the TPC. Deviation of the measured energy loss $\mathrm{d}E/\mathrm{d}x|_{\mathrm{meas}}$ from the expected $\mathrm{d}E/\mathrm{d}x|_{\mathrm{exp}}$ is calculated for each track as

$$n\sigma = \frac{1}{R} \ln \frac{\mathrm{d}E/\mathrm{d}x|_{\mathrm{meas}}}{\mathrm{d}E/\mathrm{d}x|_{\mathrm{exp}}}, \tag{1}$$

where R is the $\ln(\mathrm{d}E/\mathrm{d}x)$ resolution of the TPC. Pions are selected with the condition $|n\sigma| < 3$ and kaons $|n\sigma| < 2$. Furthermore, if a track has a matched hit in the TOF, its measured velocity β_{meas} is compared to the expected β_{exp} and the track is required to fulfill $|1/\beta_{\mathrm{meas}} - 1/\beta_{\mathrm{exp}}| < 0.03$ in order to be used in the analysis.

4. Topological reconstruction of open charm mesons

STAR equipped with the HFT is able to track charged particles with great precision and thanks to this, topological properties of D^0 meson decay are used in its reconstruction. In the analysis, firstly all pions and kaons are combined into pairs. Then, properties of this pairs are studied in order to study whether they come from D^0 meson decay. Figure 1 shows schematic decay of D^0 meson together with topological variables. D^0 is created in the place of collision, primary vertex, and decays in the secondary vertex into the pair of daughter particles (kaon and pion). Position of the secondary vertex is calculated as the point of the closest approach of these daughter tracks. Topological variables used in this analysis are:

- DCA between reconstructed daughter particles (DCA_{12}),
- decay length of D^0 meson candidate, calculated as distance between primary and secondary vertex,

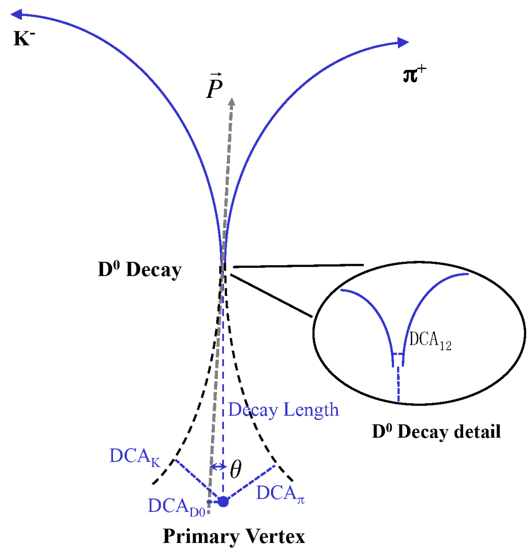

Figure 1. Schematic representation of D^0 meson decay and its topological variables: distances of the closest approach of kaon and pion to primary vertex (DCA_K and DCA_π) and between them (DCA_{12}), D^0 meson DCA to primary vertex (DCA_{D0}) and pointing angle θ between reconstructed D^0 momentum ($\vec{P}$) and decay length vector.

- kaon and pion DCA to the primary vertex (DCA_K and DCA_π),
- D^0 meson DCA to the primary vertex (DCA_{D0}),
- pointing angle θ between reconstructed D^0 momentum and decay length vector,
- angle between reconstructed D^0 momentum and kaon momentum.

5. Machine learning algorithm training

Topological properties of the pairs are used in the Boosted Decision Trees algorithm to isolate D^0 candidates in data. In this machine learning algorithm classifiers are not individual variables, but a set of binary structured decision trees constructed in the training phase of the algorithm. In the algorithm application phase, every pair is tested by the set of trees in order to classify it as signal or background. The decision of trees is then projected to the individual number - BDT response, that have values from -1 (background-like) to 1 (signal-like). In the presented analysis, BDT is trained separately in three pair (D^0) p_T intervals: 1–2, 2–3, 3–5 GeV/c.

For the algorithm training, the samples of signal and background pairs are needed as the input. Signal sample are D^0 decays generated with PYTHIA. Momenta and DCA of daughter particles from these decays are smeared in accordance with the detector response. Background sample for training are wrong(like)-sign pairs of kaons and pions ($K^-\pi^-$ and $K^+\pi^+$) from recorded data. In the training part of the algorithm, input pairs are divided to training and test samples. After the algorithm is trained and decisions trees are constructed, BDT response is calculated for all training and test pairs. Its

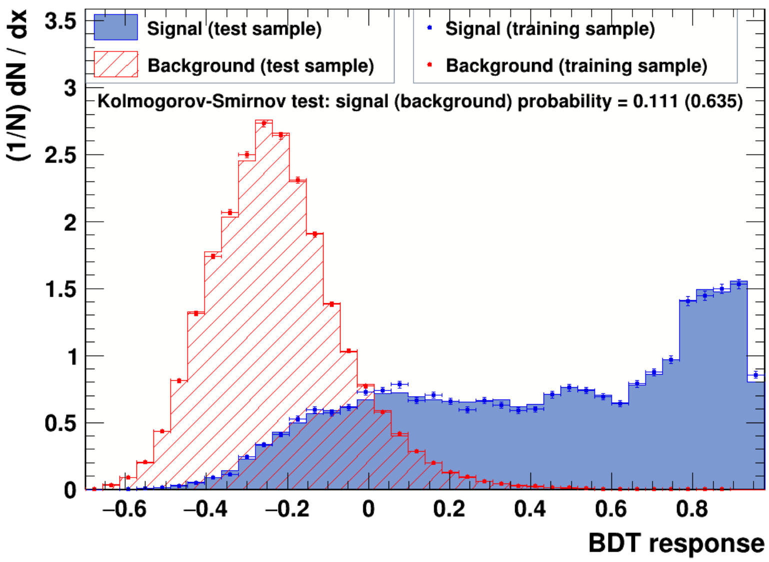

Figure 2. Boosted Decision Trees response distributions for signal and background pairs with transverse momentum $2 < p_{\mathrm{T}} < 3$ GeV/c, for both test and training samples.

distribution is shown in Fig. 2. It can be seen that the signal and background are clearly separated. In addition, since the shapes of BDT response for training and test samples are the same, the algorithm is not overtrained.

Signal and background efficiencies (ϵ_S, ϵ_B respectively) together with their purities and signal significance Σ after application of different cuts on the BDT response for pairs with $2 < p_{\mathrm{T}} < 3$ GeV/c are shown in Fig. 3. Signal significance is defined as

$$\Sigma = \frac{N_{\mathrm{S}}\epsilon_S}{\sqrt{N_{\mathrm{S}}\epsilon_S + N_{\mathrm{B}}\epsilon_B}}, \tag{2}$$

where N_{S} and N_{B} are estimates of number of signal and background pairs before BDT application. N_{S} is estimated using D^0 invariant yield measured in p+p collisions [17] and the detector reconstruction efficiency. N_{B} is evaluated from the number of wrong(like)-sign pairs in the data.

6. BDT application on data

After the machine learning method is trained, it is applied on both correct(unlike)-sign pairs and wrong(like)-sign pairs from the data and BDT response is calculated for every pair. Invariant mass distributions for pairs that fulfill the cut on BDT response are further used to evaluate the significance of signal in data. Background ($N_{\mathrm{B,data}}$) is estimated via wrong-sign pairs and then subtracted from the correct-sign combinations. Resulting invariant mass distributions of correct-sign pairs are fitted by the combination of a Gaussian function for signal and a linear function for the residual background. D^0 raw yield (Y) is extracted using the bin-counting method in the $\pm 3\sigma$ region around

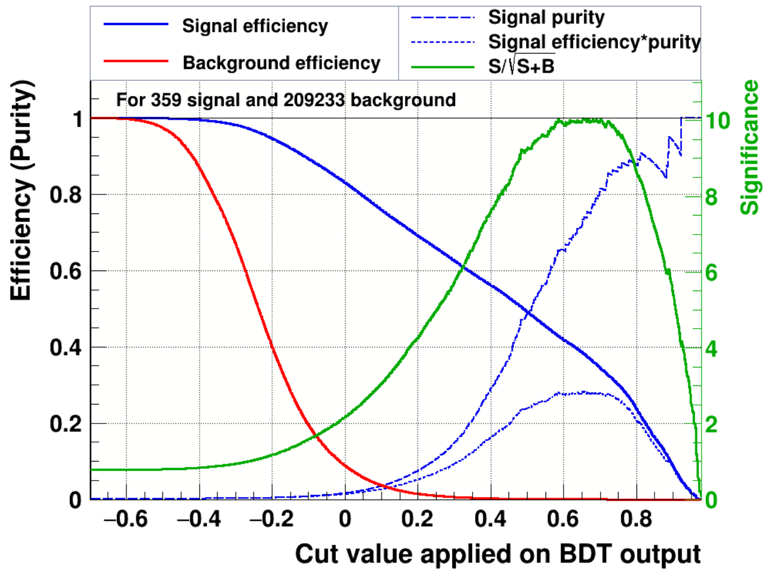

Figure 3. Evaluation of BDT response cuts performance for pairs with transverse momentum $2 < p_{\mathrm{T}} < 3$ GeV/c.

the mean of the fitted Gaussian function with residual background subtracted. Finally, signal significance in data Σ_{data} is calculated as

$$\Sigma_{\mathrm{data}} = \frac{Y}{\sqrt{Y + 2N_{\mathrm{B,data}}}}. \tag{3}$$

Multiple BDT response cuts are applied on data and significances are calculated for all of them. Resulting distributions for all tested pair p_{T} intervals are in Fig. 4. In this plot, vertical lines show the BDT response cuts, where significance calculated from BDT training (Eq. 2) is maximal in three tested D^0 p_{T} bins. It can be seen, that the BDT response cuts with maximum significance in data are consistent with those calculated in the BDT algorithm training (Fig. 3). Finally, signal significance higher than 6 is achieved in all of the tested p_{T} intervals.

7. Summary

Measurements of open charm mesons are important not only in heavy-ion collision, where QGP is created, but also in the asymmetric small systems, such as d+Au collisions, where CNM effects are investigated.

At STAR, D^0 mesons are reconstructed in d+Au collisions at $\sqrt{s_{\mathrm{NN}}} = 200$ GeV. Thanks to the HFT, topological reconstruction of hadronic decay channel is used. Furthermore, extraction of the D^0 signal has been optimized using the TMVA Boosted Decision Trees method. This machine learning method significantly helps to improve the D^0 meson measurement.

Evaluations of the efficiency corrections on D^0 raw yields and systematic

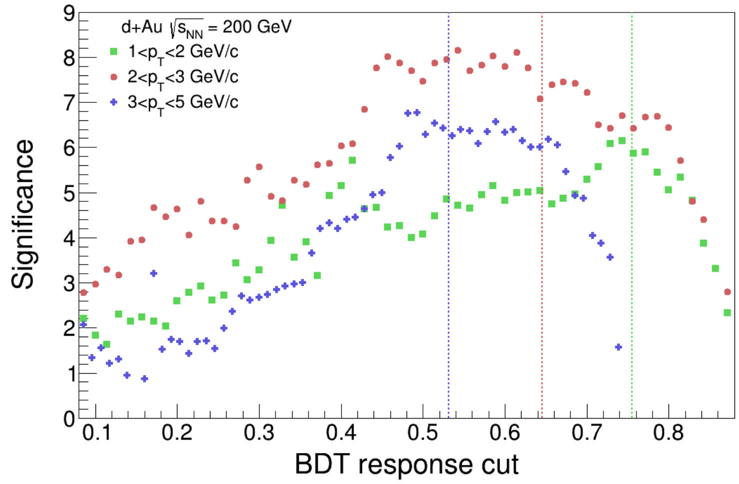

Figure 4. Significance scan of cut on BDT response on data. Vertical lines show BDT response cuts with maximum significance calculated from BDT training.

uncertainties are under way, to determine the invariant yield and nuclear modification factor of D^0 mesons in d+Au collisions.

Acknowledgment

This work was supported by the grants LM2015054 and LTT18002 of Ministry of Education, Youth and Sports of the Czech Republic.

References

[1] Adams J *et al* (STAR Collaboration) 2005 *Nucl. Phys.* A **757** 102–83
[2] Lin Z and Gyulassy M 1995 *Phys. Rev.* C **51** 2177; **52** 440(E)
[3] Adam J *et al* (STAR Collaboration) 2019 *Phys. Rev.* C **99** 034908
[4] Adamczyk L *et al* (STAR Collaboration) 2017 *Phys. Rev. Lett.* **118** 212301
[5] Noble J V 1981 *Phys. Rev. Lett.* **46** 412–5
[6] Aubert J *et al* 1983 *Phys. Lett.* B **123** 275–8
[7] Vitev I, Goldman J T, Johnson M and Qiu J 2006 *Phys. Rev.* D **74** 054010
[8] Vitev I 2007 *Phys. Rev.* C **75** 064906
[9] Adam J *et al* (ALICE Collaboration) 2016 *Phys. Rev.* C **94** 054908
[10] Adamczyk L *et al* (CMS Collaboration) 2019 CMS-PAS-HIN-19-009
[11] Tanabashi M *et al* (Particle Data Group) 2018 *Phys. Rev.* D **98** 030001
[12] Hocker A *et al* 2007 PoS(ACAT)040
[13] Anderson M *et al* 2003 *Nucl. Instrum. Methods* A **499**, 659–78
[14] Llope W J *et al* (STAR Collaboration) 2012 *Nucl. Instrum. Methods* A **661** S110–3
[15] Llope W J *et al* 2014 *Nucl. Instrum. Methods* A **759** 23–8
[16] Qiu H *et al* (STAR Collaboration) 2014 *Nucl. Phys.* A **931** 1141–6
[17] Adamczyk L *et al* (STAR Collaboration) 2012 *Phys. Rev.* D **86** 072013